RP Current Trends In Applied Sciences (e-ISSN: 2583-7486)
Vol. 5, No. 2 (April – June 2026) pp. 65–70

RESEARCH PLATEAU PUBLISHERS

Cite this article: M. Sahoo, D. Behera, Fluctuation induced electrical conductivity in YBCO/Sb_2O_3 superconductor composite, *RP Cur. Tr. Appl. Sci.* **5** (2026) 65–70.

Original Research Article

Fluctuation induced electrical conductivity in YBCO/Sb_2O_3 superconductor composite

M. Sahoo[1,*], D. Behera[2]

[1]Department of Physics, Gurugram University, Gurugram, Haryana, India
[2]Department of Physics & Astronomy, National institute of Technology, Rourkela, Odisha, India
*Corresponding author, E-mail: sahoomousumi0@gmail.com

ARTICLE HISTORY
Received: 18 April 2026
Revised: 27 May 2026
Accepted: 27 May 2026
Published: 13 June 2026

KEYWORDS
HTSC; Electrical conductivity; Grain boundary; AL model.

ABSTRACT
High-temperature superconductors (HTS) are widely used in modern technological applications because of their unique properties, like the expulsion of magnetic fields and zero electrical resistance. A series of $YBa_2Cu_3O_{7-y}$ + xSb_2O_3 superconducting samples were prepared using the solid-state reaction method. Fluctuation induced electrical conductivity of YBCO has been analysed around the superconducting transition T_c by adding Sb_2O_3. Dimensionality of fluctuation and the excess conductivity has been calculated by using Aslamazov-Larkin model fitting. The excess conductivity study reveals the transition of two dominant regions (2D and 3D) above the critical temperature T_c. 2D to 3D crossover temperature demarcates dimensional nature of fluctuation inside the grains is influenced by Sb_2O_3 incorporation in YBCO matrix. Increase in the value of coherence length and inter-layer coupling signifies that Sb_2O_3 increase the CuO_2 interlayer coupling. The structural disorder has been studied using XRD and Raman techniques.

1. Introduction

Even after several decades of research on high T_c superconductors (HTSC), these materials are still interesting for many researchers. In recent years there have been intense theoretical and experimental activities in the investigation of the copper oxide based high T_c superconductors [1-3]. Bulk HTSC samples are granular in nature, characterized by the presence of grains and twin boundaries, secondary phases and other defects. Granular superconductors can be considered as disordered systems formed by anisotropic grains weakly coupled and randomly distributed, where we can distinguish two main contribution to their properties. The first one, called intragrain contribution, is associated with high critical current density values and grains completely shielded at sufficiently low magnetic fields. The second one, called intergrain contribution, is characterized by lower critical current density values associated to Josephson couplings. Hence the granularity arising from this structure, is responsible for the typical low J_c values of HTSC and for their strong dependence with temperature and applied magnetic field. Therefore, the intergrain material has an important role in the technological applications of HTSC, in particular in the presence of magnetic fields [4-6]. The planes containing copper and oxygen atoms that are chemically bonded to each other have a crucial importance in YBCO. The existence of the Cu-O chains and the CuO_2 planes in cuprate superconductors indicates the important role of Cu atoms. Thus, the ionic radius as well as the valence number of the dopant element has a crucial role in determining the characteristics of new superconductors. Doping of YBCO with various elements is conducted for two basic purposes. The first one is the modification of the microstructure in order to obtain fundamental information related to the possible mechanisms, and the second one is to improve its physical characteristics. It has been seen that substitutions at the Y and Ba sites does not generate any discernible effect, while substitution at the Cu and O sites has significant effects on the superconducting properties of cuprates [7]. Due to the low melting point and the possible surfactant action of semi-metallic Sb_2O_3 doping, it is expected that doping with Sb could improve the grain boundary characteristics and enhance the intergranular coupling in Y_{123}. Paulose et al. [8] reported that Sb_2O_3 doping significantly increases the rate of oxygen absorption in the Y_{123} system. Jin et al. [9] determined that Sb_2O_3 doping of Y_{123} improves the value of the critical current density J_c along with a decrease in T_c and a reduction in grain size with increasing porosity. In this paper, an attempt has been made to analyze the Superconducting Order Parameter Fluctuation (SCOPF) behavior with temperature dependent electrical resistivity ρ (T) around the superconducting transition T_c in (1 – x) YBCO + x Sb_2O_3 (x = 0.0, 0.01, 0.03, 0.05, 0.08, 0.2 wt. %) composites. The superconducting transition can be described in the framework of Ginzburg-Landau (GL) theory, in terms of the complex superconducting order parameter ψ (r). The mean value $<\psi(r)>$ is zero in the normal state and is different from zero in the superconducting state, below the transition temperature T_c, where $|\psi(r)|^2$ is related to the density of Cooper pairs. The dimensional fluctuations of SCOPF for the composite samples has been analyzed by using Aslamazov-Larkin (AL) theory. Because of layer separation and the temperature dependent out-of-plane coherence length ξ (T), the SCOPFs in the HTSC can exhibit either a two dimensional (2D) or a three dimensional (3D) or a crossover behavior. The

order parameter dimensionality (OPD) or a crossover depends on the temperature range [10].

2. Experimental procedure

YBCO powder is prepared by the solid-state reaction route by mixing stoichiometries amount of Y_2O_3, $BaCO_3$, CuO followed by grinding, calcination, sintering and annealing respectively. A series of polycrystalline composite samples of $(1 - x)$ YBCO + x Sb_2O_3 (x = 0.0, 0.01, 0.03, 0.05, 0.08, 0.2 wt. %) were ground and pressed into pellets. The composite pellets were sintered at 920° C for 12 hours and then cooled to 500° C where they were kept for 5 hours in an oxygen atmosphere for oxygen intake. Temperature dependent resistivity $\rho(T)$ was measured using the standard four-probe techniques.

3. Results and discussion

3.1 Temperature dependence of resistivity

Measurements of the resistivity dependence of temperature for different samples with various amounts of Sb_2O_3 are shown in figure1. The resistive transition exhibits two different regimes. The first is characterized by the normal state that shows a metallic behaviour above $2T_c$. The normal state resistivity follows Anderson and Zou relation $\rho_n(T) = A + BT$. Where $\rho_n(T)$ is calculated by using the values of A and B parameters, which are obtained from the linear fitting of resistivity in the temperature range $2T_c$ to 300 K and extrapolated to 0 K gives resistivity slope ($d\rho/dT$) and residual resistivity ρ_0 respectively (Fig.1). Second is the region characterized by the contribution of Cooper pairs fluctuation to the conductivity below T_c, where $\rho(T)$ is deviating from linearity. This is mainly due to the increasing rate of cooper pair formation on decreasing the temperature. Therefore, the fluctuation induced conductivity in this region follows the AL model to yield the dimensional exponent appropriately to fluctuation-induced conductivity. The normal state resistivity of the low and the high % doped sample is higher than that of pure sample which is tabulated in Table 1. At the temperature value T_{c0} the electrical resistivity vanishes and the phase of the order parameter acquired long range order between the grains of the system. This critical temperature signifies the coherence transition. A finite tailing is observed in the superconducting transition for all the Sb_2O_3 added samples before the resistance attains zero value. It indicates that the superconducting grains get progressively coupled to each other by Josephson tunneling across the grain boundary weak links. The zero-resistance at the temperature T_{c0}, characterizes the onset of global superconductivity (where all the grains become superconducting i.e intragrain as well as grain boundaries becomes superconducting) in the samples where the long-range superconducting order is achieved. At 0.2 % addition of Sb_2O_3 a purely semiconductor type behavior was observed.

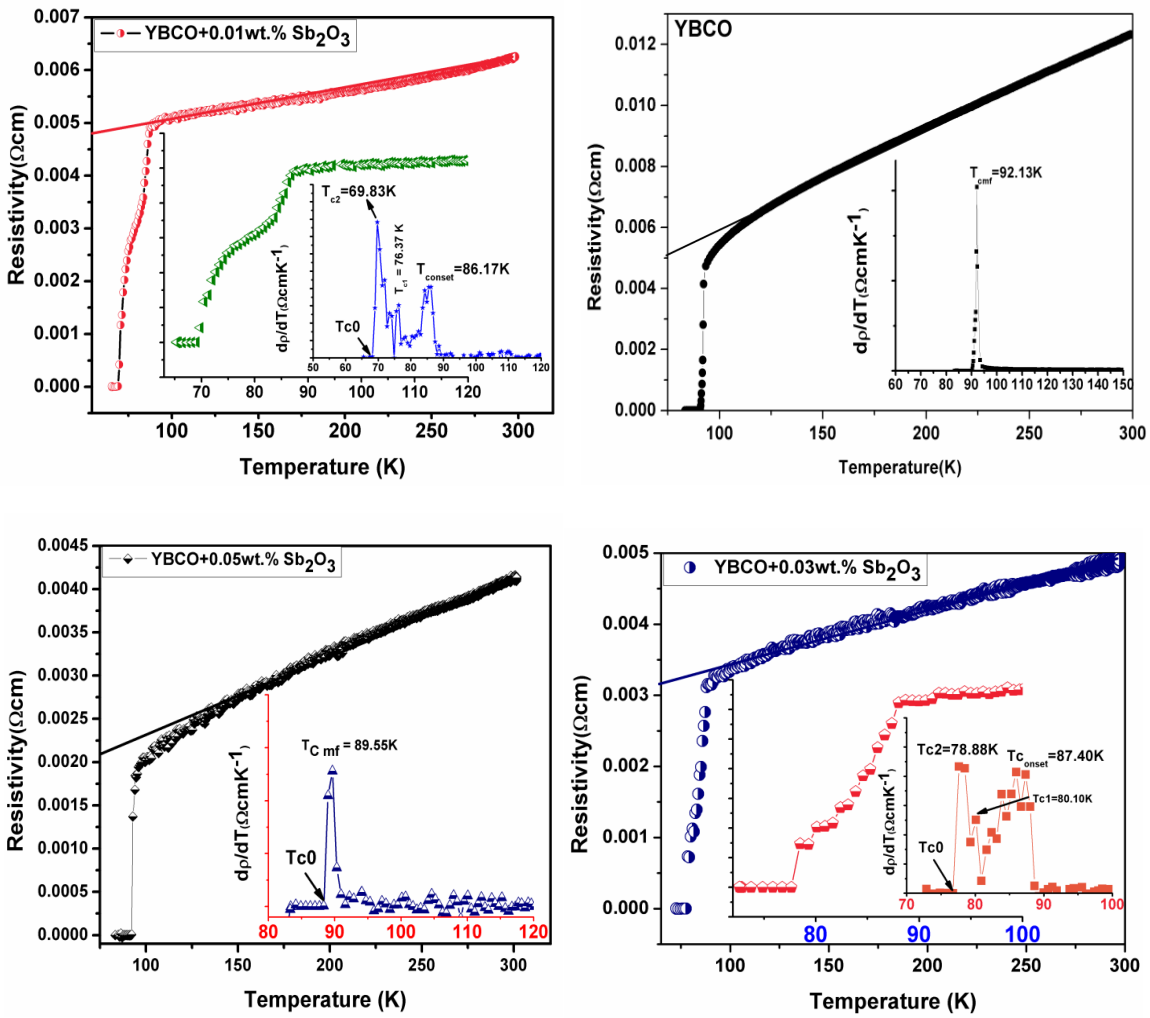

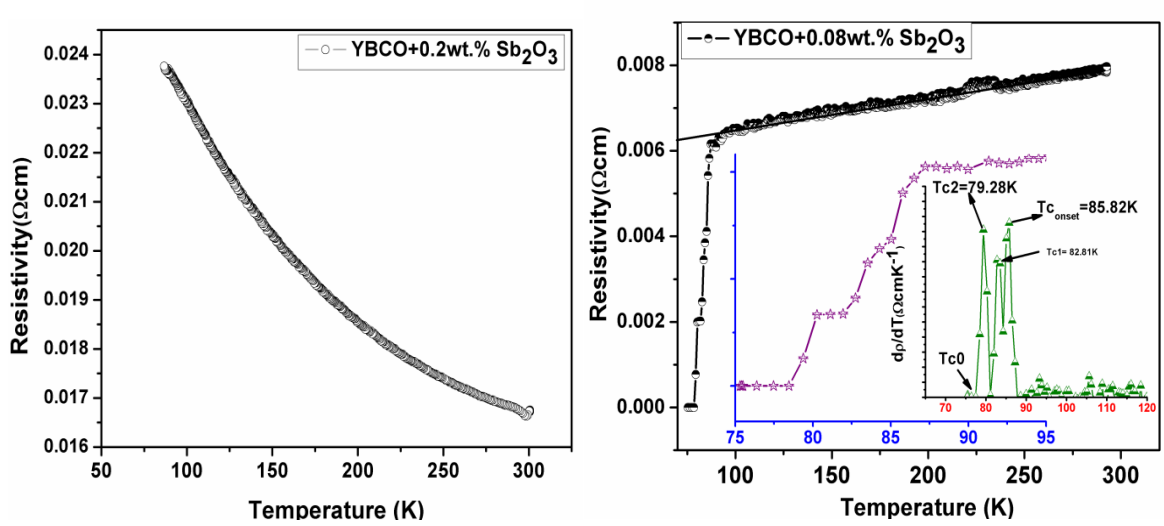

Figure 1: Resistivity dependences on the temperature for YBCO+ x Sb_2O_3 (x= 0.0, 0.01, 0.03, 0.05, 0.08, 0.2 wt. %) composites.

Table 1: Variation of normal state and superconducting parameters in the composites with different Sb_2O_3 wt.%.

Sb_2O_3 (wt.%)	T_{c0} (K)	T_{c2} (K)	T_{c1} (K)	T_{conset} (K)	ΔT_c (K)	α_n	$\rho_n(0)$ (μΩ.cm)	ρ_{wl} (μΩ.cm)	ρ_P (μΩ.cm)	$\alpha_{stru.}$
0.00	90.32	92.13	…	98.00	0.04	1.80	0.01	3100	49.6	1033
0.01	67.17	69.90	76.37	86.17	0.20	2.73	0.08	4340	320	1446
0.03	76.76	78.88	80.10	87.40	0.10	1.24	0.07	2860	140	953.33
0.05	87.68	89.79	…	96.00	0.09	2.11	0.05	1590	50	530
0.08	77.46	79.28	82.81	85.82	0.18	2.14	0.07	5810	350	1936

From the temperature derivative of resistivity plots (shown in the inset graph of Fig. 1) firstly, we observe a sharp peak at T_c, which is related to intragranular fluctuation. These characteristic fluctuations define the so-called pairing transition [11]. The temperature value corresponding to this maximum peak is close to the bulk critical temperature T_c followed by hump or secondary peak which broadens for composite samples. In all the composite samples a broading and step like structure was found in the resistivity plot below the superconducting transition (inset graph Fig. 1). One more point is noticed that the superconducting transition temperature splits into two (revealed as double peaks in the $d\rho/dT$ plot) T_{c1} and T_{c2} along with a broadening of overall transition temperature. This was also reported by Azhan et al in Sb_2O_3 doped BSCCO superconductor [12]. Such behavior is accounted to the weak-link nature of granular superconductors as the latter is composed of superconducting grains embedded in a non-superconducting host. Out of the two superconducting transition temperatures, the higher one (T_{c1}) marks the superconductivity in grains whereas the grain boundary still remains normal and the lower one (T_{c2}) when the grain boundary also becomes superconducting. Transition at T_{c1} manifests significant amount of strongly coupled grains and the zero-resistance state is achieved when the Josephson tunneling between the grains, forms a connected superconducting path across the entire sample at T_{c2} as the temperature is lowered. The appearance of additional transition temperature T_{c2} and its broadening clearly reflects that the Sb_2O_3 added, goes to the grain boundary region, and becomes superconducting only due to proximity effect at lower temperatures. The transition width (ΔT_c) defined as full width half maxima increases with doping concentration. This may be due to the gradual occurrence of non-superconducting additional phases and the effect of microscopic inhomogeneity. The percolation factor 'α_n' arising due to current frustration caused by misalignment of anisotropic grains and sample defects such as voids and cracks are estimated from the temperature coefficient of resistivity $d\rho/dT$. This factor contributes to percolate conduction in granular copper oxides. Generally, in the normal-state electrical conduction of granular samples, current path frustration and meandering of current may occur due to two mechanisms. One is associated with the orientational disorder of anisotropic grains [13]. It depends on the degree of texturization, and has its origin in the extreme anisotropy of the copper oxides, the in-plane resistivity ρ_{ab} being orders of magnitude less than the out of plane resistivity ρ_c [14]. As we assume that due to the extreme conduction anisotropy, current blocks along the pathways with misaligned grains and current percolates through the sample along unobstructed paths, which results in a cross section reduction and path lengthening [15] that increases resistivity by a multiplicative factor, denote as $1/f$ $(0 < f \leq 1)$. Another source of resistivity enhancement comes from structural defects of the grains (i.e pores, isolating boundaries, microcracks etc.) denoted as $1/\alpha_{str}$ $(0 < \alpha_{str} \leq 1)$. Besides the percolative processes, a contribution to resistivity coming from the intergrain barriers ρ_{wl} is to be added. So, the observed resistivity can be written as:

$$\rho_n = (1/\alpha_n)(\rho_{ab} + \rho_{wl}) \quad (1)$$

where α_n is a shorthand for

$$\alpha_n = f \,.\, \alpha_{str} \quad (2)$$

and it may be referred to as the normal-state percolative factor. The normal-state resistivity of polycrystalline HTS is linear with temperature. This linearity of ρ_n enables determination of the two sample parameters α_n and ρ_{wl}. Taking temperature derivatives of the equation (1) and assuming ρ_{wl} constant we can get [16, 17]

$$\alpha_n = \rho'_{ab} / \rho'_n \quad (3)$$

where the primes stand for temperature derivatives. Similarly, from Eqs. (1) and (3)

$$\rho_{wl} = \rho'_{ab}/\ \rho'_n\ \rho_n(0) = \alpha_n\ \rho_n(0) \quad (4)$$

where ρ_n (0) is the extrapolation of the normal state resistivity to zero temperature. Based on single crystal measurements ρ_{ab} is assumed [18] to vary linearly with temperature (ρ'_{ab}= 0.5 μΩ.cm.K^{-1}) with a negligible zero-temperature intercept. For typical polycrystalline Y-based HTSC α_n is in the range 0.2-0.05. The main difference between percolation in the normal state and in paracoherent state is that in the latter the orientational disorder is irrelevant as the grain resistivity becomes vanishingly small both in the ab plane and the c direction, resulting in the loss of anisotropy. Once bulk grains go superconducting (but the intergrain junctions remain normal) nothing hinders conduction along that path. Only the structural quality factor α_{str} and the intergrain resistivity ρ_{wl} enter the paracoherent resistivity ρ_p ,

$$\rho_p = (1/\ \alpha_{str})\ \rho_{wl} \quad (5)$$

From eq (2) and (4)

$$\rho_p = f\,\rho_n(0) \quad (6)$$

The relation should be $\rho_n(0) > \rho_p > \rho_{wl}$. For YBCO ρ_p should be equal to approximately one-third of the normal-state resistivity extrapolated to zero temperature [19]. The decrease in the value of ρ_{wl} and the increase in the value of T_{c0} will indicate the better connectivity of grains. In our samples for 0.01wt.% added sample the value of weak-link resistivity increases to a greater extent and then starts decreasing for 0.03, 0.05 wt.% added sample. The reverse thing is happening in the value of T_{c0}. This confirms the better connectivity between grains in 0.03 and 0.05 % composite samples. The increase in the value of α_n will indicate better grain alignment and elimination of voids and cracks in the composites. The grain size might increase. The value of α_n is higher in the composite samples as compared to the pristine sample. The cracks and voids are less in 0.01, 0.02 and 0.05wt.% added samples and the grain size slightly increase in the higher wt.% Sb_2O_3 added samples.

3.2 Excess conductivity

3.2.1 Theoretical background

In the absence of an external magnetic field, the total conductivity above T_{c0}, can be expressed in a combination of three terms as follows,

$$\sigma = \sigma_n + \sigma_{AL} + \sigma_{MT} \quad (7)$$

The above eq^n states that, above T_{c0}, the conductivity is enhanced above the normal state conductivity (σ_n) by the fluctuation conductivity of both the Aslamzov-Larkin (LD) term (σ_{AL}) and the Maki-Thompson term (σ_{MT}). The MT term has been usually ignored in the analysis of various zero-field fluctuation conductivity measurements, because of the general belief that the intrinsic large inelastic scattering rates in these materials would reduce significantly the contribution of the MT term to the fluctuation conductivity. Also, as the ceramic HTSC are in the dirty superconductor limit, the MT contribution is probably negligible in zero-applied magnetic field [20-22]. Since it has been well known that YBCO has a quasi-two-dimensional nature as well as the characteristics of dimensional crossover as a function of temperature, we adopt Aslamazov-Larkin (AL) model to analyze the excess conductivity. The density of states (DOS) at the Fermi energy contribution introduced by Tewordt and coworkers by using a quasi-two-dimensional tight binding model is better adapted to copper-oxide HTSC. But this may introduce variations in the excess conductivity amplitude 'A'. But all these effects are being taken directly into account in our approximation for normal state resistivity (ρ_n).

According to AL theory the excess-conductivity ($\Delta\sigma$) above T_c generated by the thermodynamic fluctuations [23] diverges as a power-law given by

$$\Delta\sigma = A\varepsilon^{-\lambda} \quad (8)$$

$\Delta\sigma$ is defined by

$$\Delta\sigma = (1/\rho - 1/\rho_R) = \sigma(T) - \sigma_R(T) \quad (9)$$

where ρ and ρ_R are the measured and normal resistivity, σ (T) is the measured conductivity and σ_R (T) is the extrapolated conductivity under the assumption of a linear behavior of temperature dependent resistivity. The reduced temperature $\varepsilon = (T-T_c)\ /T_c$, defined with respect to the mean field critical temperature (T_c) of the normal to superconducting transition. λ is the Gaussian critical exponent depending on the dimensionality of the HTSC system. The dimensionality D of the fluctuation system is related through the expression

$$\lambda = 2 - D/2. \quad (10)$$

The effective value of the critical exponent for 3D and 2D are $\lambda = 0.5$ and $\lambda = 1$ respectively [24]. The values of A for 3D and 2D are $A = e^2/32\hbar\xi\ (0)$ and $e^2/16\hbar d$ respectively. '$\xi(0)$' is the zero-temperature coherence length or GL correlation length and 'd' is the effective separation of CuO_2 layers. These relations are based on GL theory and are valid only for the mean field temperature region ($1.01T_c$ to $1.1T_c$). Lawrence and Doniach (LD) [25] extended the AL model for layer superconductors, where conduction occurs mainly in 2D CuO_2 planes and these planes are coupled by Josephson tunneling. The excess conductivity parallel to the layers in the LD Model is given by

$$\Delta\sigma\ (T)_{LD} = e^2/16\hbar d\varepsilon\{1+(2\xi(0)/d)^2\ \varepsilon^{-1}\}^{-1/2} \quad (11)$$

From equation (11) at Temperature close to T_c, $2\xi(0)/d >> 1$ and $\Delta\sigma(T)$ diverges as $\varepsilon^{-1/2}$ which corresponds to 3D behavior. Whereas at $T >> Tc$, $2\xi(0)/d << 1$ and $\Delta\sigma(T)$ diverges as ε^{-1} which corresponds to 2D behavior.

Figure 2 displays the logarithmic Plot of excess conductivity as a function of reduced temperature (ε). In order to explain the experimental data with theoretical predicted ones, the different regions of the plot were linearly fitted and the exponent values (λ) were determined from the slopes. Four different fluctuation regions are clearly distinguishable, which can be identified as the critical, 3D, 2D and 1D regions. λ is the conductivity exponent, which equals - 0.5 for the 3D region,-1 for the 2D region, and -1.5 for the 1D region fluctuations.

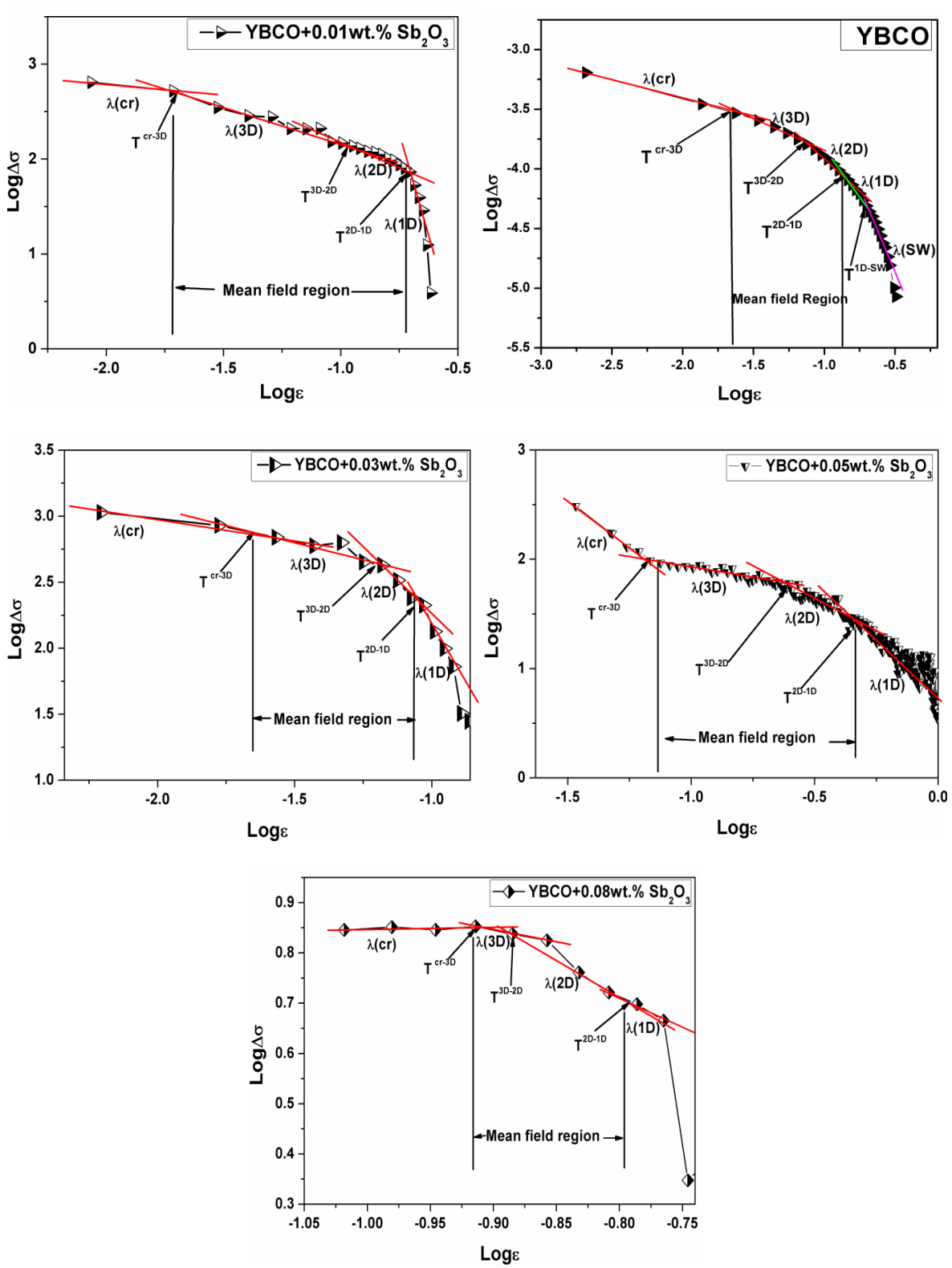

Figure 2: log–log plot of excess conductivity $1/\rho - 1/\rho_R$ as a function of reduced temperature $\epsilon = (T-T_c)/T_c$ in YBCO+ *x* Sb_2O_3 composites.

Table 2: Sb_2O_3 content dependence of different cross over temperatures.

Sb_2O_3 (wt.%)	λ (3D)	λ (2D)	λ (1D)	λ (SW)	T^{cr-3D} (K)	T^{3D-2D} (K)	T^{3D-2D} (K)	T^{1D-SW} (K)	$\xi_c(0)$ (A^0)	J
0.00	-0.52	-1.20	-1.48	-3.2	92.11	96.21	101.9	108.51	1.22	0.043
0.01	-0.55	-0.94	-1.80	…	71.24	76.99	83.66	…	1.85	0.100
0.03	-0.44	-1.09	-1.26	…	80.11	83.12	84.56	…	1.34	0.052
0.05	-0.55	-0.86	-1.80	…	90.93	111.11	130.30	…	2.83	0.234
0.08	-0.48	-1.28	-1.53	…	89.30	89.97	92.62	…	2.13	0.133

From the above data it can be seen that the 3D region is lies in the lower temperature region, for all the composite samples as compared to the pristine sample. The coherence length $\xi_c(0)$ is higher in the composite samples as compared to the pristine sample which is highest for the 0.05 wt.% added sample. Accordingly the inter-layer coupling $J = [2\ \xi_c(0)]^2/d^2$ is higher in the composite samples as compared to the pristine and highest for the 0.05wt.% added composite. This means that the added Sb_2O_3 increase the CuO_2 interlayer coupling.

4. Conclusion

The effect of semiconductor Sb_2O_3 on the fluctuation conductivity is studied. The different regions observed are the critical region at $T < T_c$, the mean field region at T close to T_c and the short-wave fluctuations at $T > T_c$. The experimental data fit with theoretical predicted ones. It is found that T_{c0} decreases and the transition width ΔT_c increases with the increasing Sb_2O_3 content which signifies the degradation of inter-grain weak links. T_{LD} lies in the lower temperature region, for all the composite samples as compared to the pristine sample. This signifies that fluctuation of copper pairs in 3D is dominated in the samples. The coherence length and inter-layer coupling is higher in the composite samples as compared to the pristine. This means that the added Sb_2O_3 increase the CuO_2 interlayer coupling.

Authors' contributions

The author read and approved the final manuscript.

Conflicts of interest

The author declares no conflict of interest.

Funding

This research received no external funding.

Data availability

No new data were created.

References

[1] E. Dagotto, Correlated electrons in high-temperature superconductors, *Rev. Mod. Phys.* **66** (1994) 763–840.
[2] A.P. Kampf, Magnetic correlations in high temperature superconductivity, *Phys. Rep*. **249** (1994) 219–351.
[3] D.J. Scalapino, The case for dx^2–y^2 pairing in the cuprate superconductors, *Phys. Rep*. **250** (1995) 329–365.
[4] F.M. Araujo-Moreira, W.A. Ortiz, O.F. de Lima, Multilevel granular structure and its coupling distribution in melt-textured $YBa_2Cu_3O_{7-x}$, *Physica C* **311** (1999) 98–106.
[5] F.M. Araujo-Moreira, W.A. Ortiz, O.F. de Lima, Study of the intergranular and intragranular characteristics in a melt-textured-growth sample of $YBa_2Cu_3O_{7-x}$, *Physica C* **205** (1994) 235–240.
[6] F.M. Araujo-Moreira, W.A. Ortiz, O.F. de Lima, Exponential critical state model applied to ac susceptibility data for the superconductor $YBa_2Cu_3O_{7-\delta}$, *J. Appl. Phys.* **80** (1996) 3390–3395.
[7] J.M.S. Skakle, Crystal chemistry substitutions and doping of $YBa_2Cu_3O_x$ and related superconductors, *Mater. Sci. Eng. R* **23** (1998) 1–40.
[8] K.V. Paulose, J. Koshy, P. Uma Devi, A.D. Damodaran, High temperature superconductivity in air quenched $YBa_2Cu_3O_{7-\delta}$ doped with Sb_2O_3, *Appl. Phys. Lett*. **59** (1991) 1251–1253.
[9] S. Jin, T.H. Tiefel, R.A. Fastnacht, G.W. Kammlott, Critical current behavior in the Sb_2O_3-doped $YBa_2Cu_3O_{7-\delta}$ superconductor, *Appl. Phys. Lett*. **60** (1992) 3307–3309.
[10] A.V. Pogrebnyakov, L.D. Yu, T. Frello, P. Vase, In-plane paraconductivity in c-oriented epitaxial $YBa_2Cu_3O_{7-x}$ films above T_c , *Physica C* **183** (1991) 27–31.
[11] J. Roa-Rojas, R.M. Costa, P. Pureur, P. Prieto, Superconducting fluctuation studies in $YBa_2Cu_3O_{7-x}$, *Phys. Rev. B* **61** (2000) 12457–12462.
[12] H. Azhan, K. Azman, S.Y.S. Yusainee, The role of antimony (Sb) addition on BSCCO superconductor, *Solid State Sci. Technol*. **17** (2009) 215–221.
[13] J.W. Ekin, A.I. Braginski, A.J. Panson, M.A. Janocko, D.W. Capone, N.J. Zaluzec, B. Flandermeyer, O.F. de Lima, M. Hong, J. Kwo, S.H. Liou, Evidence for weak link and anisotropy limitations on the transport critical current in bulk polycrystalline $Y_1Ba_2Cu_3O_x$, *J. Appl. Phys.* **62** (1987) 4821–4828.
[14] T.A. Friedmann, M.W. Rabin, J. Giapintzakis, J.P. Rice, D.M. Ginsberg, Direct measurement of the anisotropy of the resistivity in the a-b plane of twin-free single-crystal superconducting $YBa_2Cu_3O_{7-\delta}$, *Phys. Rev. B* **42** (1990) 6217–6221.
[15] J. Halbritter, Percolation in superconducting cuprates: Resistivity and critical currents, *Int. J. Mod. Phys. B* **3** (1989) 719–732.
[16] S.S. Bungre, R. Meisels, Z.X. Shen, A.D. Caplin, Are classical weak-link models adequate to explain the current-voltage characteristics in bulk $YBa_2Cu_3O_7$, *Nature* **341** (1989) 725–727.
[17] E. Babić, M. Prester, Z. Marohnić, T. Car, N. Biskup, S.A. Siddiqui, Critical currents and differential resistance of $YBa_2Cu_3O_{7-x}$ superconducting ceramics, *Solid State Commun.* **72** (1989) 753–757.
[18] B. Batlogg, Physical properties of cuprate superconductors: An introduction, in: Physics of High-Temperature Superconductors, Springer-Verlag, Berlin (1992) pp. 219–238.
[19] A. Diaz, J. Maza, F. Vidal, Anisotropy and structural-defect contributions to percolative conduction in granular copper oxide superconductors, *Phys. Rev. B* **55** (1997) 1209–1215.
[20] S. Hikami, A.I. Larkin, Magnetoresistance of high temperature superconductors, *Mod. Phys. Lett. B* **2** (1988) 693–698.
[21] A.G. Aronov, S. Hikami, A.I. Larkin, Zeeman effect on magnetoresistance in high-temperature superconductors, *Phys. Rev. Lett*. **62** (1989) 965–968.
[22] K. Maki, R.S. Thompson, Fluctuation conductivity of high TcT_cTc superconductors, *Phys. Rev. B* **39** (1989) 2767–2770.
[23] L.G. Aslamazov, A.I. Larkin, The influence of fluctuation pairing of electrons on the conductivity of normal metal, *Phys. Lett. A* **26** (1968) 238–239.
[24] X.G. Tang, Q.X. Liu, J. Wang, H.L.W. Chan, Electric-field dependence of dielectric properties of sol-gel derived $Ba(Zr_{0.2}Ti_{0.8}O_3$ ceramics, *Appl. Phys. A* **96** (2009) 945–952.
[25] J. Lawrence, S. Doniach, Theory of layered superconductors, Proc. 12th Int. Conf. on Low Temperature Physics, Kyoto, Keigaku, Tokyo (1970) p. 361.